# Synthesis and Characterization of rGO doped $RuO_2$ nanocomposites for Photocatalytic and Antioxidant Properties

Guruswamy K[1], Kishore N Gujjar[2*], Munirajappa N N[3], Narasimha S A[4], Nagaraja N[5], Krishna Mohan R[6], Nagaraja D[7]

[1, 2*]Department of Physics, IDSG Government College, Chikmagaluru, Karnataka, India-577102
[3]Department of Physics, Government Science College, Nrupathunga University, Bengaluru, Karnataka, India -560001
[4]Department of Physics, Government First Grade College, Koppa, Karnataka, India-577126.
[5,6]Department of Physics, Maharani's Science College for Women (Autonomous) Mysore, Karnataka, India-570005
[7]Department of Chemistry, Government Science College Chitradurga, Karnataka, India.

***Corresponding Author:** Kishore N Gujjar
*Department of Physics, IDSG Government College, Chikmagaluru, Karnataka, India-577102, E-mail: kishoregujjarn@gmail.com

**Abstract:**
Recently, electrochemical energy storage has arisen to be one of the major areas of research to deal with the exorbitant energy demands of the modern civilization. Hasty modernization has amplified the demand for sustainable energy, and fuel cells have received much devotion for power generation based on renewable energy. Fuel cells have the competence of green technology as the electric energy generation from chemicals produces no combustion [1]. Consequently, beside fuel cells and battery technology, fascinating and challenging results observed in the recent past, during materialization of supercapacitors have triggered sharp increase in research proclivity to re-enter this aspect of renewable and sustainable energy storage technology. The performances of Supercapacitors mainly reliant on electrode materials, nature of electrolyte used and the range of voltage window hired. The unusual properties of Carbon-based electrode materials, such as widespread surface area, electrical conductivity, and faster electron transmission kinetics with low production cost. But their specific capacitances are found to be too low for commercialization. Ruthenium dioxide ($RuO_2$) owing to its high theoretical specific capacitance value has been generally predictable as promising materials for supercapacitor devices but high production cost, agglomeration effects stand as high non-invasion fence for commercial practice. Accordingly, $RuO_2$ based nanocomposites have been widely studied to minimize the material cost, with real-time enhancement in the electrochemical performances [2-3].
In this paper, an effective synthesis of rGO-$RuO_2$ composite for electrochemical sensor studies has been reported. The modified Hummer's method was used to produce reduced graphene oxide (rGO). The ruthenium dioxide ($RuO_2$) was introduced to the rGO via the hydrothermal method to form the composite. X-ray diffraction (XRD), scanning electron microscopy (SEM) and Fourier transform infrared spectroscopy (FTIR) were used to examine the sample. The CV measurements show a significant improvement in electrochemical reversibility, with the specific capacitances of rGO and rGO/$RuO_2$ being 45 and 110 $Fg^{-1}$, respectively. These results indicate that the capacitive behaviour and electron transfer of the rGO/$RuO_2$ nanocomposite was significantly higher than that of rGO. The charge-discharge curves show good symmetry and linear deviations with time change, indicating superior capacitance. This is primarily due to the electrode reversible reaction, and it has also been revealed as a type of super capacitor electrode material. The electrode materials obtained have the highest specific capacitance and excellent rate capability.

**Keywords:** rGO/$RuO_2$, Photocatalysis, antioxidant, composites, sensor.

## 1. Introduction:

Industry and research centres around the world are coping to report the world-wide energy demand and are competing with all existing substitute technologies. Super capacitors signify an attractive substitute for portable electronics and automotive applications due to their high specific power and long life. In fact, the growing demand of portable systems and hybrid electric vehicles, memory protection in complementary metal-oxide-semiconductor (CMOs), logic circuit, vapour-compression refrigeration system (VCRs), CD players, PCs and UPS in security alarm systems, remote sensing, smoke detectors etc. require high power in short term pulses. “Reduced graphene oxide (rGO)-metal oxide” nano composite is the trending field, with applications in super capacitors, batteries, photocatalytic dye degradation, tracing and absorption of heavy and toxic elements, firefighting coatings, biosensors and electrocatalysts in oxide fuel cells. Many studies have noticed that rGO nano composite materials decorated with metals, have enhanced properties that are absent in their individual

components. The functionalization of metal oxide nanocomposite on the graphene matrix improves the performance of metal oxide nano composite, which exhibit properties like agglomeration and Ostwald ripening. The composite of graphene with metal oxides like $RuO_2$, $SnO_2$, $MnO_2$, $Co_3O_4$, $V_2O_5$, $Fe_2O_3$ among these "$Ruo_2$" have proved the enhancement of electrochemical and pseudo capacitance behaviour by overcoming the limitations such as reduced electrical conductivity, poor electrochemical cycling ability and low specific capacitance. A hybrid system consisting of graphite cathode and $RuO_2$ anode has been tested for suitability as a hybrid supercapacitor. Shishun Qi et al. studied the photocatalytic applications of graphene nanocluster decorated niobium oxide nano fibres [1-2]. Wang et al. [3] reported the fabrication of hybrid electrochemical capacitor with binder-free $RuO_2$/graphene and studied the electrochemical characteristics with the discharge specific capacity of 58 Fg-1 at 0.1 Ag-1. $RuO_2$ anchored grapheme nanocomposite has been synthesized with low amount of graphene content with the capacitance value of 34 Fg-1 at 0.05Ag-1. rGO/$RuO_2$ based pseudo capacitive electrode for asymmetric supercapacitor has been reported by Kong et al. with a specific capacitance value of 80 Fg-1 at 0.2 Ag-1. Amongst the most significant TMOs, $RuO_2$, owing to its high conductivity, superior electrochemical reversibility and high-valued specific capacitance in cooperation with large cycle efficacy has been widely considered for supercapacitor application [4]. In addition, RuO2 has been extensively used as positive electrode material for Li-ion batteries in the past years [5]. Outstanding electrocatalytic features of RuO2 in several electrochemical processes have also been reported recently [6]. Basically, $RuO_2$ is the oxide of Ru in +4 oxidation state. Ruthenium, a member of platinum group metals, is transition metal element capable of exhibiting variable oxidation states [7]. Ruthenium is stable in nature although it lies among the less common ones on the earth's crust. The stable solid phase anhydrous oxide of ruthenium mainly adopts the "rutile structure" of RuO2, although it is found to exist in other different forms with respect to water hydration [8]. Electrical resistivity data of $RuO_2$ is reported to be 35.2 ± 0.5 μΩ-cm under ordinary conditions which indicates high conductivity compared to other transition metal oxides and superior charge transport properties originate from the delocalized metal-metal states of $RuO_2$ [9]. The molecular orbital (MO) theory successfully explained the thermodynamic stability as well as high isotropic charge transport characteristics of $RuO_2$ [10].

In the present investigation, the synthesis and characterization of rGO/$RuO_2$ nanocomposite and their Photocatalytic, antioxidant and chemical sensor properties has been studied by using hydrothermal method.

**2. Characterization**:

i) X – Ray diffraction studies of rGO and rGO/$RuO_2$ nano composites are carried out using a high-resolution X – Ray diffractometer maxima – 7000 (Shimandzu) at a scanning rate 20 $min^{-1}$ using CuKα radiation (λ = 1.54 Å) operating at 40 kV and 30 mA.

ii) Morphology of the rGO and rGO/$RuO_2$ nano composite was studied by using SEM (SU 1500, HITACHI). The accelerating potential was 15 kV and the beam current was 20mA. The powdered sample was dispersed in water and then the sediment was dried at room temperature before gold coating.

iii) The energy dispersive X-Ray studies of rGO and rGO/$RuO_2$ were studied using Topcon ABT-32 SEM which consist of an iXRF systems silicon drift (SDD) light element X-Ray detector of 30mm sensor area and 133 eV resolution.

iv) The presence of functional group identification analysed for the rGO and rGO/$RuO_2$ and FTIR spectrum was recorded on Perkin Elmer FTIR 1650 spectrophotometer at ambient temperature using KBr disc method. The disc containing 0.0010 gm of the sample and 0.3000 of fine grade KBr was scanned with 16 scans at wave number range of 400 to 4000 $cm^{-1}$.

**3. Materials and Methods:**

The materials used for the entire work with all the specifications, purity, grades, structural and chemical formulas with supplier names are mentioned in the Table

**Table 1. Details about the chemicals used**

| Materials | Formula | Specifications | Suppliers |
|---|---|---|---|
| Sodium Nitrate | $NaNO_3$ | Molar mass: 84.90g/mol | Merck, Bengaluru |
| Sulphuric acid | $H_2SO_4$ | Molar mass: 39.90g/mol | Sigma, Aldrich |
| Hydrogen peroxide | $H_2O_2$ | Molar mass: 34.01g/mol | Merck, Bengaluru |
| Potassium Permanganate | $KMnO_4$ | Molar mass: 158.0g/mol | Merk, Bengaluru |
| Ruthenium chloride | $RuCl_3$ | Molar mass: 207.43g/mol | Merk, Bengaluru |
| Tri-Sodium citrate | $Na_3C_6H_5O_7$ | Molar mass: 294.10g/mol | Sigma, Aldrich |
| Sodium sulphite | $Na_2SO_3$ | Molar mass: 126.0g/mol | Merk, Mumbai |
| Ammonia | $NH_3$ | Molar mass: 17.031g/mol | Sigma, Aldrich |
| Ethyl alcohol | $CH_3CH_2OH$ | Molar mass: 46.07 g/mol | Merk, Bengaluru |

### 3.1 Synthesis of rGO by Hummers Method:

Almost 60 years after the introduction of Staudenmaier's strategy, chemists Hummers and offeman in Mellon Institution of Industrial Research developed a different recipe for making GO. A water free mixture of concentrated sulphuric acid, sodium nitrate, and potassium permanganate was prepared and maintained below 45°C for graphite oxidation. According to their description, the whole oxidation process finished within 2hours, leading to a final product with higher degree of oxidation than Staudenmaier's product. However, it was found that Hunmmers product usually has an incompletely oxidized graphite core with GO shells, and a pre-expansion process is helpful to achieved higher degree of oxidation. First introduced by Kovtyukhova in 1999, a pre-treatment of graphite with an 80 °C mixture of concentrated $H_2SO_4$, $K_2S_2O_8$ and $P_20_5$ for several hours was widely adopted thereafter. The pre-treated mixture was diluted, filtered, washed and dried before the real Hummers Oxidation step took place. Later on, it was found that if graphite samples have smaller flake size or have been thermally expanded, the Kovtyukhova pre-treatment can be Skipped. Other reported modifications also include increase of the amount of potassium permanganate, etc. Nowadays, this modified Hummers method is the most common recipe used for GO preparation. A typical GO product made by this method consists of thin flakes of GO with 1nm in thickness (corresponding to a single layer) and around 1 μm in lateral dimensions on average, meanwhile the chemical composition was determined to be C: 0: H = 4:2.95:2.5. [11-13].

### 3.2 Preparation of rGO/$RuO_2$ nanocomposites:

In a typical synthesis process, 0.1 M of $RuCl_3H_2O$ in 50 ml of water was thoroughly mixed with rGO solution (As prepared rGO powder of 5 mg was mixed with 20 ml of water) under stirring condition in magnetic stirrer for 1 hour. The rGO powder work exfoliated via continuous stirring to produce rGO nanoplatelets the freshly prepared $NH_3$, $H_2O$ solution was used to maintain the pH seven and stirred continuously at room temperature to obtain rGO/$RuO_2$ precursor solution. Next the mixture was transferred to a 100 ml RB flask, reflux for about 3 hours then it was cooled at room temperature overnight. Filtration followed by several times with alcohol, dried in the hot air oven at 150°C for about 20 minutes. Then the obtained powder was grinded well in the form of fine powder and then used for many applications, characterization and other studies [13-14].

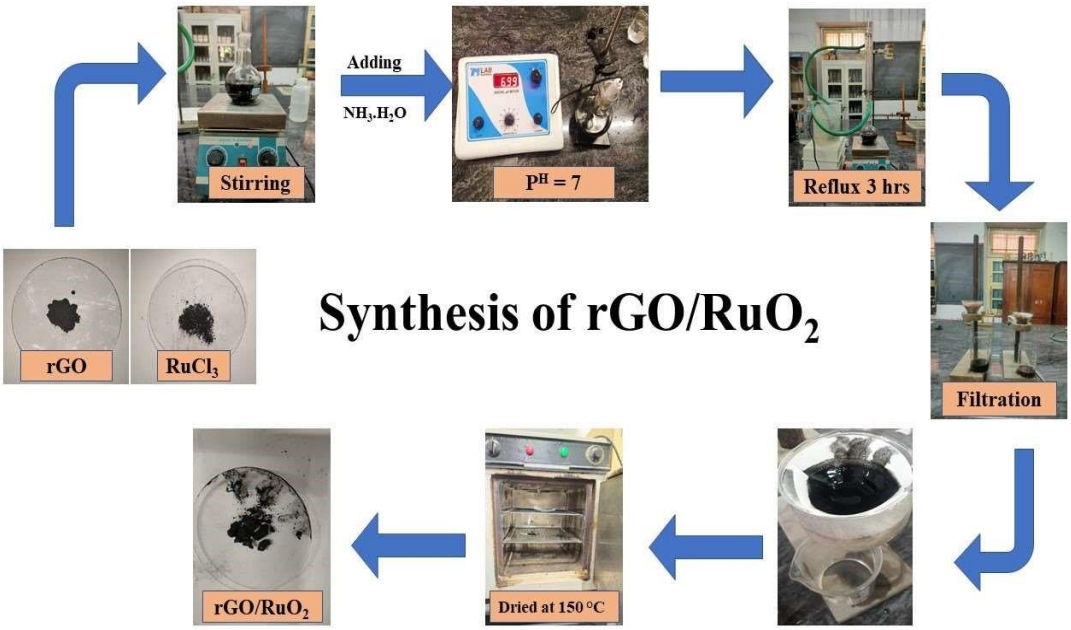


### 4. Results and Discussion:

### 4.1 X-Ray diffraction studies:

The phase composition and the crystallinity of the powder was detected by X-ray diffractometer using the Shimadzu-7000 X-ray diffractometer with monochromatized Cu-Kα radiation. The XRD of rGO and $RuO_2$/rGO were shown in Fig. 1 (a) and (b). The peaks shown in the XRD pattern of rGO/$RuO_2$ are more intense and sharper, representing good crystallinity of the prepared sample. No evidence of impurity peaks was detected, which indicated that high purity. The strong and narrow peak signifies that the product has well crystalline nature of particles. X-ray Diffraction is the primary tool for the characterization of Nanoparticles. XRD studies provide details on crystallinity and phase purity of the rGO with lattice planes (002) and (111). The prepared rGO/$RuO_2$ indicates the hexagonal structure with lattice planes (110), (101) and (220) respectively. The average crystallite sizes of particles were assessed in agreement with Debye Scherrer's equation.

$$\mathbf{D} = \frac{\mathbf{K\lambda}}{\boldsymbol{\beta} - \mathbf{cos\theta}}$$

Where $\boldsymbol{D}$ is the size of crystallite; $\boldsymbol{K}$is a dimensionless shape factor, with a value close to unity (shape factor has a typical value about 0.9); $\boldsymbol{\lambda}$ is the X-ray wavelength; $\boldsymbol{\beta}$ is Full width at half maximum intensity; $\boldsymbol{\theta}$ is the Bragg angle.

The $\boldsymbol{\theta}$ values are:

a) rGO: (002) $\theta$ = 27.228; (111) $\theta$ = 54.283.

b) rGO/$RuO_2$: (110) $\theta$ = 27.381; (101) $\theta$ = 34.384; (220) $\theta$ = 56.449.

From XRD, the average crystalline sizes of rGO and and rGO/$RuO_2$ were found to be 17 to 27 nm.

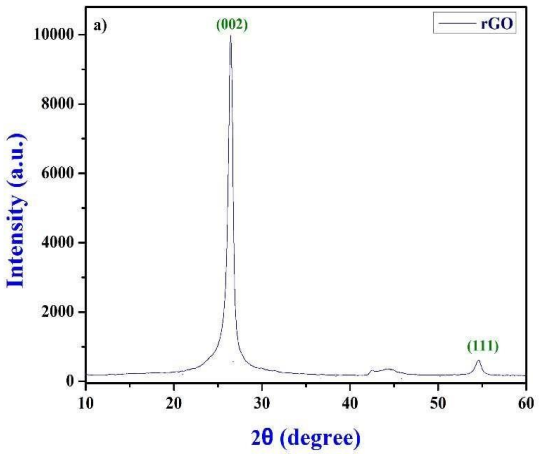


Fig.1. (a) XRD pattern of rGO

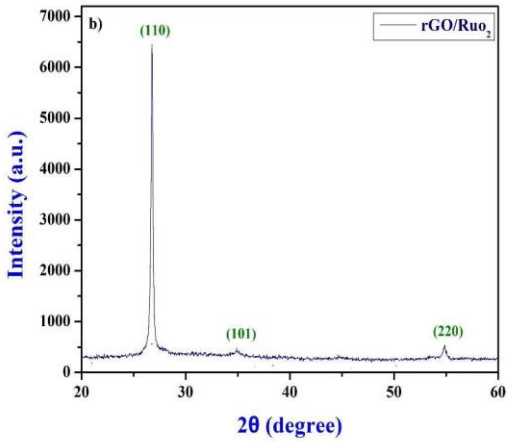


Fig.1 (b) XRD pattern of rGO/$RuO_2$

**4.2 Scanning Electron Microscope (SEM):**

SEM examination was used to observe the surface morphology of the rGO and rGO/$RuO_2$ nano particles as shown in Fig.2(a) and Fig.2(b). SEM images of $RuO_2$ nano particles revealed in the Fig.2 (b) clearly show that particles look like cluster and a cylindrical structure. The appearance of larger nano particles is due to Vander Waals clusters of smaller entities and magnetic interactions among the particles. Fig.2(a) demonstrates a uniform structure and hexagonal shape for rGO nano particles. However, in some places, the size of particles is bigger, and they are agglomerated by different clusters. In addition, it demonstrates the rGO/$RuO_2$ nano particles are well dispersed in the powder sample.

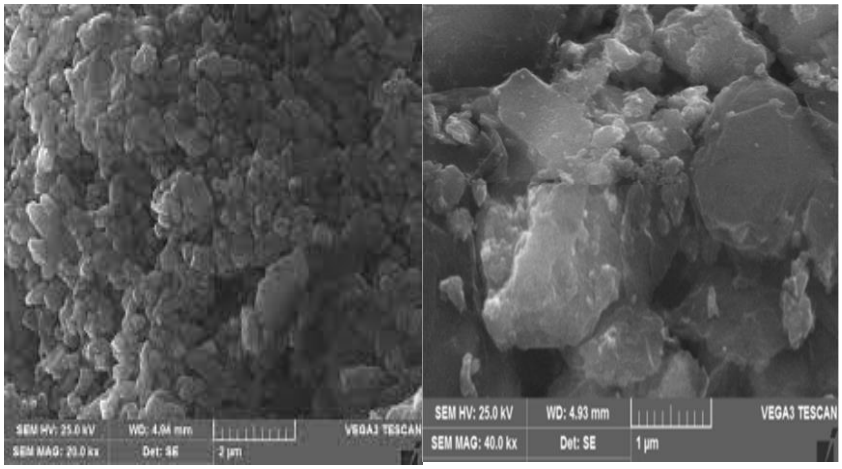


**Fig.2 a**) SEM images of rGO and b) rGO/ $RuO_2$ nano Composite

**4.3 Energy Dispersive X-Ray Analysis (EDX):**

EDX analysis was used to assess the elemental composition of rGO/$RuO_2$ nanoparticles is as show in Fig. (3), it depicts irregular and unequal $RuO_2$ nano particles with average diameters ranging from 10 to 200 nm, suggesting that particle sizes are more similar with smaller agglomerations of the grain size. The EDX pattern infers the presence of elements Ru, C and O. The weight percentage of Ru, C and O were indicated in the Fig. (3).

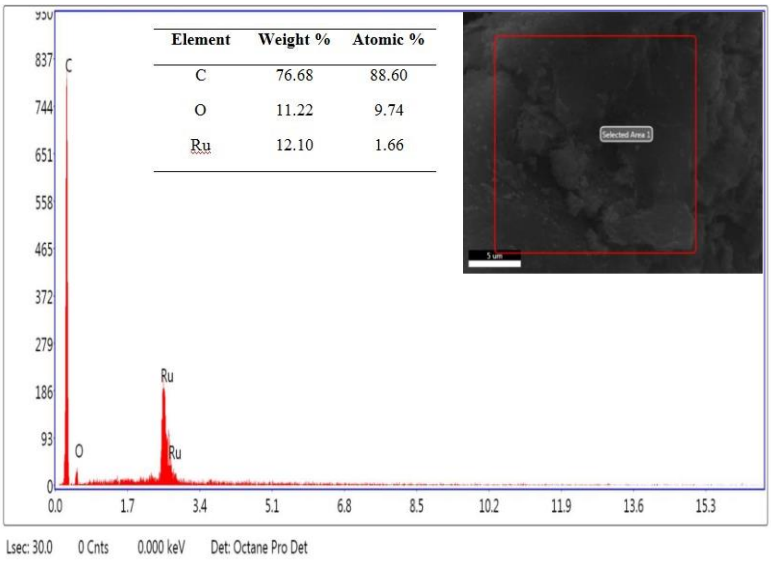


**Fig.3.** EDX for rGO/$RuO_2$

### 4.4 Fourier transforms infra-red spectrometer studies:

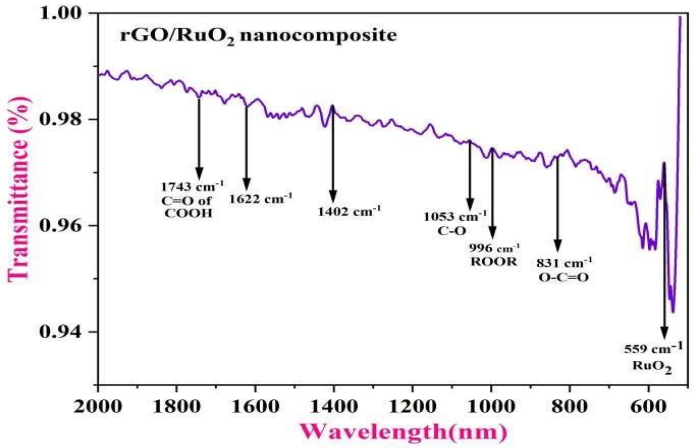


Fig.4. FTIR spectra of rGO/$RuO_2$ nano composite

FT-IR study was performed in the wavelength range 500–2000$cm^{-1}$, to identify the presence of bending or stretching vibrations in the deposited ruthenium oxide sample. Fig.4 shows the FTIR spectrum of the rGO/$RuO_2$ nano composites prepared by reflux method. Spectrum comprises of two transmittance peaks. The characteristic features of oxides appear below 1200$cm^{-1}$. The FT-IR transmittance spectrum gives information about phase, composition as well as the way by which oxygen is bound to the metal ions (M–O structure). Fig.2 shows the FT-IR absorption spectrum of $RuO_2$ thin film. The characteristic vibrational mode of rutile $RuO_2$ band is observed at 559 $cm^{-1}$. peaks due to carboxy C–O (1053 $cm^{-1}$), peroxy O–C=O (831 cm-1), peroxo ROOR (996 $cm^{-1}$), and C=O of COOH (1743 $cm^{-1}$). For the $RuO_2$/rGO nanocomposites prepared by reflux method, the peak intensities for the oxygen functional groups were reduced significantly, and the peak for C=O (1743 $cm^{-1}$) was virtually removed. It can be inferred that $Ru^{3+}$ ions were associated with and eliminated most of the oxygen-containing groups, such as COOH peaks (1743 $cm^{-1}$), whereas the peak at 1622 $cm^{-1}$ for the skeletal vibration of the graphene sheets remained. The peak intensities of C–O stretching vibrations (1053 $cm^{-1}$), carboxy C–O were decreased. This suggests that GO can be reduced to rGO by in situ chemical synthesis (introduction of Ru ions), without reducing agents such as hydrazine or sodium borohydride.

### 4.5 Photocatalytic degradation of Orange-G by rGO and rGO/$RuO_2$ nano powders:

The photo degradation performances of prepared photocatalysts for Orange-G dye under UV-Visible light were measured and the UV-Visible absorption spectra are as shown in Fig.5 and Fig.6. The photocatalytic tests for $RuO_2$ and rGO/$RuO_2$ nanocomposite photocatalysts (60 mg) were conducted with Orange-G of 20 ppm with time duration of 100 min under UV light irradiation. Finally, the absorbance was measured for these collected dye samples in the range of 500 nm. The photocatalytic activity of rGO/$RuO_2$ nano- composite

samples showed the enhanced photo degradation (87.1%) under UV-Visible light irradiation than the rGO (67.3%) nanoparticles. The photo degradation performances of photocatalysts depend on the size of particles, morphology and surface properties. The crystallite sizes of prepared rGO and rGO/$RuO_2$ nanocomposite photocatalysts from chemical combustion method were 42nm and 39.85 nm respectively, observed from PXRD data. Therefore, the decrease in crystallite size showed improved photocatalytic activity due to low recombination rate and high interfacial charge transfer. The photo degradation efficiency of synthesized rGO/$RuO_2$ photo- catalyst on dye was measured for every 20 min time interval. The photo degradation of dye gets started quickly after absorption of UV- visible light, produces electrons and holes in Valence band. The electrons are able to move from Valence band to conduction band, which provokes the enhanced photo-catalytic activity of dye degradation. The generated electrons are transferred to the photocatalyst and start reacting with the atmospheric $O_2$ to form superoxide radicals. Further, number of active radicals were produced by the effect electron produces superoxide radicals ($O_2$•—) and holes in the Valance band will react with water ($H_2O$) converted into hydroxyl radicals (OH•—). These formed radicals are reacting with the dye which it undergoes degradation.

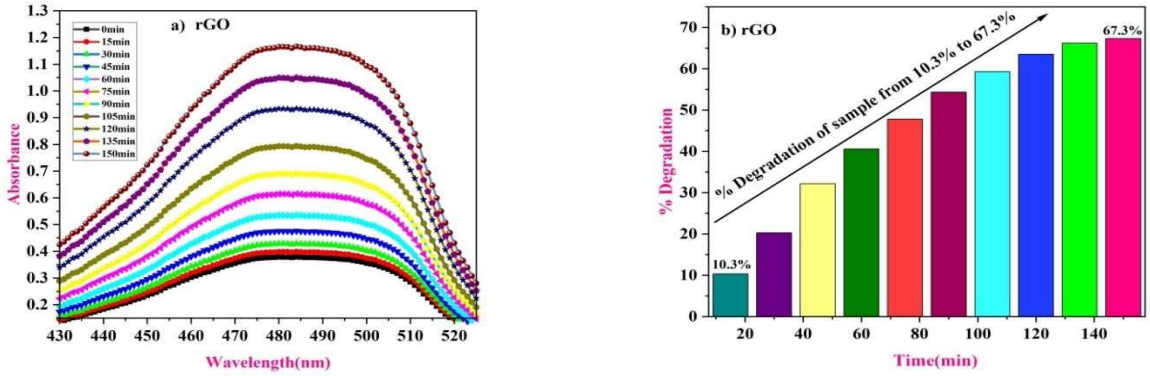


**Fig.5** UV-Visible spectra of rGO

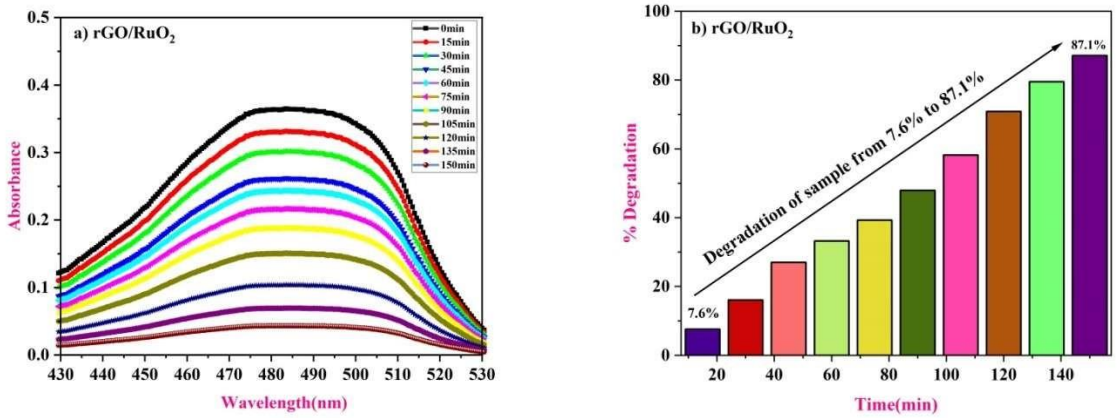


Fig.6 UV-Visible spectra of rGO/$RuO_2$

**4.6 Antioxidant property of rGO/$RuO_2$ by DPPH method:**

A DPPH test was used to evaluate the antioxidant activity of rGO/$RuO_2$ nano particles. DPPH was prepared by dissolving it in methanol and adding it to samples in different concentrations. The tubes were incubated at 25°C for 1hour before being measured for absorbance at 517 nm with an Elico UV 1800 spectrophotometer (Fig.7). We calculated the concentration (g/ml) of each fraction required to eliminate 50 % of the free radicals in a particular amount of time. Add varied amounts of solution to each of the five consecutively labelled test tubes (100 mL, 200 mL, 300 mL, 400 mL, and 500 mL). Add methanol to the test tubes with a small pipette. Add 2cc of the freshly prepared DPPH solution to each test tube and then wrap them in aluminium foil to keep them from drying out. Allow it to sit in the dark for about an hour. Measure the absorbance of the solution with a UV-Visible spectrophotometer. As a consequence, the following proportion of activity was determined. The percentage of antioxidant property was calculated using following relation (1).

$$\textbf{\% of Antioxidant activity} = \frac{\mathbf{Ac - As}}{\mathbf{Ac}}$$

Where 'Ac' is the absorbance of the control and 'As' is the absorbance of the sample.

**Table.2. Antioxidant activity of rGO nano particle.**

| Volume of extract (µL) | Volume of methanol (µL) | Concentration | Absorbance | % activity | IC50 (mg/mL) |
|---|---|---|---|---|---|
| 100 | 500 | 1000 | 1.51 | 15.1 | 67.03 |
| 200 | 400 | 2000 | 0.436 | 43.6 | |
| 300 | 300 | 3000 | 0.444 | 44.4 | |
| 400 | 200 | 4000 | 0.477 | 47.7 | |
| 500 | 100 | 5000 | 0.835 | 83.5 | |
| control | 600 | - | 2.0899 | 40.82 | |

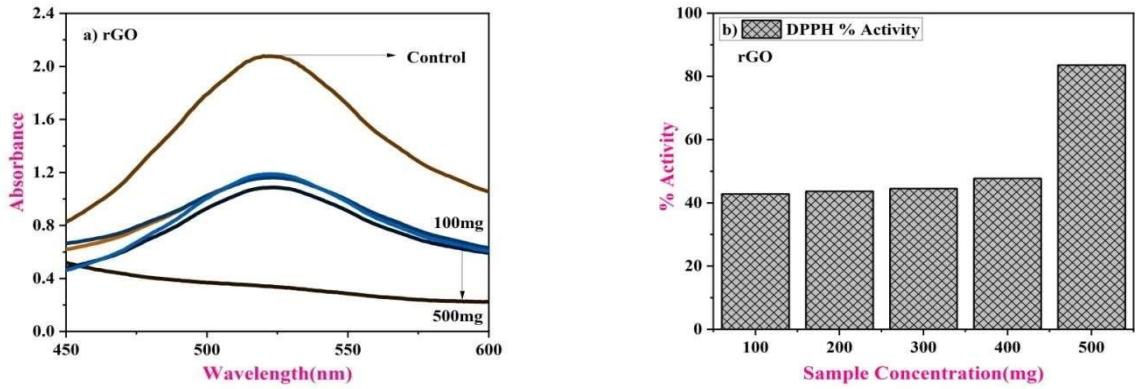


Fig.7. a) UV absorption spectrum of rGO b) Antioxidant activity of rGO.

**Table.3. Antioxidant activity of rGO nano particle.**

| Volume of extract (µL) | Volume of methanol (µL) | Concentration | Absorbance | % activity | IC50 (mg/mL) |
|---|---|---|---|---|---|
| 100 | 500 | 1000 | 0.7017 | 70.17 | 271.39 |
| 200 | 400 | 2000 | 0.718 | 71.8 | |
| 300 | 300 | 3000 | 0.8161 | 81.61 | |
| 400 | 200 | 4000 | 0.8812 | 88.12 | |
| 500 | 100 | 5000 | 0.8937 | 89.37 | |
| control | 600 | - | 2.08 | - | |

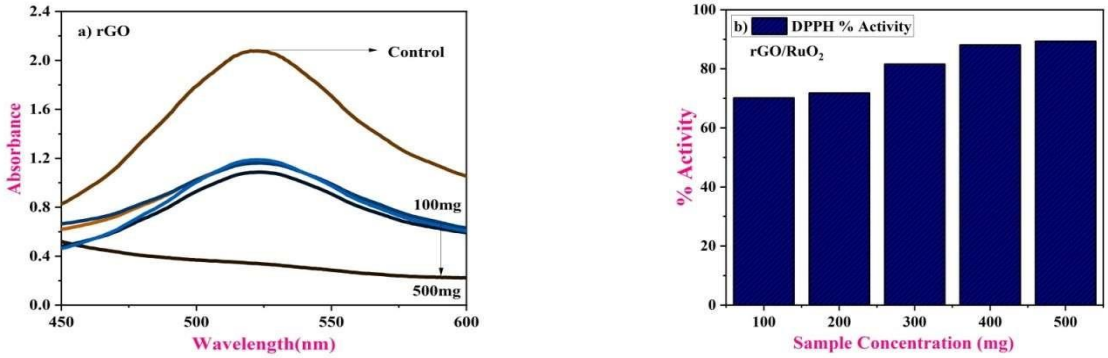


**Figure.8** a) UV absorption spectrum of rGO/$RuO_2$. b) Antioxidant activity of rGO/$RuO_2$

The UV absorption spectrum and antioxidant properties of rGO and rGO/$RuO_2$ nano particles are represented in Figures 7(a),7(b) and 8(a), 8(b) respectively. The methods for calculating antioxidant activity and the IC50 value are shown in Tables 2 and 3. The radical scavenging activities of rGO and rGO/$RuO_2$ nano particles were found to be 67.03 mg/ml, and 271.39 mg/ml respectively. The IC50 value designates the sample concentration required to scavenge 50% of the free radicals.

**Conclusion:**

The rGO and rGO/$RuO_2$ were synthesized by eco-friendly hydrothermal method and due to its lenience, cost-effectiveness and successful retrieval of rGO and rGO/$RuO_2$ nano composite. XRD analysis confirms the nano size of the composite material i.e the average crystallite sizes of rGO and rGO/$RuO_2$ were found to be 17 to 27nm. It has better photocatalytic activity under UV light which is predominantly due to its smaller size, vacancy and charge separation. The rGO/$RuO_2$ nanocomposite successfully photo decomposes acid orange G dye compound in water and a DPPH was used to assess the antioxidant activity of rGO/$RuO_2$.

**Scope for the future work:**

- Used as a catalyst for removal of toxic dyes from aqueous solution.
- Used as adsorbent for removal of toxic element present in the waste water.
- Used as photo catalyst and electrochemical sensor applications.
- Pseudo capacitance applications.

**References:**


1. Dipanwita; Majumdar; Thandavarayan Maiyalagan, Zhongqing Jiang: Chem Electro Chem: 10.1002/celc.201900668.
2. Shishun Qi, Linfeng Fei, Ruzhong Zuo, Yu Wang and Yucheng Wua: J. Mater. Chem. A,2014,2,8190–8195
3. X. Wang, Y. Guo, L. Yang, M. Han, J. Zhao, X. Cheng, Environ. Anal. Toxicol. 2012, 2, 1000154. 1-7.
4. H Xia, Y. S. Meng, G. Yuan, C Cui, L. Lu, Electro chem. Solid State Lett. 2016,15, A60–A63.
5. L.L Zhang, X. S. Zhao, Chem. Soc. Rev 2009, 38(9), 2520-2531.
6. H Over, Chem. Rev. 2012, 112, 3356−3426. J. P. Zheng, P. J. Cygan, T.R. Jow, J. Electro chem. Soc.,1995, 142, 2699–2703.
7. H. E. Suess, H. C. Urey, Abundances of the Elements. Reviews of Modern Physics 1956, 28(1), 53–74.
8. S Trasatti., G Buzzanca., Journal of Electroanalytical Chemistry, 1971,29(2), A1–A5.
9. W. D. Ryden, A. W. Lawson, C. C. Sartain, Phys. Rev. B1970, 1(4), 1494.
10. Z Fang, M A. Outlaw, D A. Dixon Journal of Physical Chemistry A2017, 121 (40), 7726 7744.
11. Kim H, Lim H-D, Kim S-W, Hong J, Seo D-H, Kim D-C, Jeon S, Park S, Kang K. 2013 Scalable functionalized graphene nano-platelets as tunable cathodes for high-performance lithium rechargeable batteries. Sci. Rep. 3, 1506–1513.
12. Guo Y, Sun X, Liu Y, Wang W, Qiu H, Gao J. 2012 One pot preparation of reduced graphene oxide (RGO) or Au (Ag) nanoparticle-RGO hybrids using chitosan as a reducing, stabilizing agent, their use in methanol electrooxidation. Carbon 50, 2513–2523.
13. K. Praveena, K. Sadhana, S.R. Murthy, Mater. Res. Bull. 2012, 47, 1096-1103.
14. C.W. Liu, C.H. Lin, J. Am. Ceram. Soc. 2007, 90, 3349-3352.
15. Hummers WS, Offeman RE. 1958, J. Am. Chem. Soc. 80, 1339.
16. B. J. Li and H. Q. Cao, J. Mater. Chem., 2011, 21, 3346–3349. 44 J. G. Hou, S. Q. Jiao, H. M. Zhu and R. V. Kumar, Cryst Eng Comm, 2011, 13, 4735–4740.
17. S. D. Zhuang, X. Y. Xu, B. Feng, J. G. Hu, Y. Pang, G. Zhou, L. Tong and Y. X. Zhou, ACS Appl. Mater. Interfaces, 2014, 6, 613–621.
18. Y. Q. Dai, Y. B. Sun, J. Yao, D. D. Lin, Y. M. Wang, H. Long, X. T. Wang, B. P. Lin, T. Y. H. Zeng and Y. S. Sun, J. Mater. Chem. A, 2014, 2, 1060–1067.
19. S. Yang, P. Zong, X. Ren, Q. Wang, X. Wang, ACS Appl. Mater. 2012, Interfaces 4 6891-6900.
20. V. Chandra, J. Park, Y. Chun, J.W. Lee, I.C. Hwang, K.S. Kim, ACS Nano. 2010, 4 3979-3986.
21. J. Guo, W.W. Tjiu, J. Pan, T. Liu, J. Hazard Mater. 2012, 225-226, 63-73.
22. H. Du, z. Wang, Y. Chen, Y. Liu, Y. Liu, B. Li, X. Wang, H. Ca, RSC Adv. 2015 5 10033-10039.
23. X F.N. Azad, M. Ghaedi, K. Dashtian, M. Montazerozohori, S. Hajati, E. Alipanahpour, RSC Adv. 2015, 5, 61060-61069.
24. Wang, Y. Guo, L. Yang, M. Han, J. Zhao, X. Cheng, Environ. Anal. Toxicol. 2012, 2, 1000154. 1-7.
25. M. Roosta, M. Ghaedi, F. Yousefi, experimental design, RSC Adv. 2015, 5, 100129100141
26. M. Dastkhoon, M. Ghacdi, A. Asfaram, Tyagi, S. Agarwal, V.K. Gupta, Sep. Purif. Technol. 2015, 156, 780-788.
27. A.A. Bazrafshan, S. Hajati, M. Ghaedi, RSC Adv. 2015, 5, 79119-79128.
28. M. Ghaedi. Reza Rahimi, A.M. Ghaedi, I. Tyagi, S. Agarwal, V.K. Gupta, J. Colloid Interface Sci. 2016, 461, 425-434.
29. A. Asfaram, M. Ghaedi, A. Goudarzi, M. Rajabi, Dalton Trans.2015, 44, 1470714723.
30. Wei L, Mao Y. 2016, Int. J. Hyd. Energy 41, 11 692– 11 699.
31. Ke Q, Liu Y, Liu H, Zhang Y, Hu Y, Wang J. 2014, RSC Adv. 4, 26 398– 26 406.

32. Paranthaman V, Sundaramoorthy K, Chandra B, Muthu SP, Alagarsamy P, Perumalsamy R. 2018, Phys. Status Solidi A 215, 1800298.
33. D Majumdar, S K. Bhattacharya Journal of Applied Electrochemistry,2017,47(7), 789-801.
34. D Majumdar, M Mandal, S K Bhattacharya, ChemElectroChem, 2019, 6, 1623 (2019).
35. (a) A. Noori, M. F. El-Kady, M. S. Rahmanifar, R. B. Kaner, M. F. Mousavi, Chem. Soc. Rev., 2019,48, 1272-1341. (b) N Choudhary, C Li, J Moore, N Nagaiah, L Zhai, Y Jung, J Thoma, Adv. Mater. 2017, 29, 1605336.
36. H Xia, Y. S. Meng, G. Yuan, C Cui, L. Lu, Electrochem. SolidState Lett. 2016,15, A60–A63.
37. Y Kim, J Yoon, G. O Park, Park, KimS. B., H., J.M Kim, W. S. Yoon, Journal of Power Sources 2018, 396,749-7
38. S Chalupczok, P Kurzweil, H Hartmann, C Schell International Journal of Electrochemistry; 2018, Article ID 1273768, 15 pages.
39. I-L Chen, Y-C Wei, T-Y Chen, C-C Hu, T- L Lin. Journal of Power Sources 2014, 268, 430 438.
40. A Noori, M F. El-Kady, M S. Rahmanifar, R B. Kaner, M F. Mousavi Chem. Soc. Rev., 2019, 48, 1272—1341
41. F.N. Azad, M. Ghaedi, K. Dashtian, S. Hajati, A. Goudarzi, M. Jamshidi, New J. Chem. 2015, 39, 7998-8005.

DOI: https://doi.org/10.15379/ijmst.v8i2.3752